
ELSEVIER
Volume 48, issue 7, July 2009
ISSN 1290-0729
International Journal of Thermal Sciences
Founded as Revue Générale de Thermique in 1962

International Journal of Thermal Sciences 48 (2009) 1392–1397

Contents lists available at ScienceDirect

International Journal of Thermal Sciences

www.elsevier.com/locate/ijts

Artificial neural networks to correlate in-tube turbulent forced convection of binary gas mixtures

Gerardo Diaz [a,*], Antonio Campo [b]

[a] School of Engineering, University of California Merced, P.O. Box 2039, Merced, CA 95344, USA
[b] University of Texas at San Antonio, Department of Mechanical Engineering, One UTSA Circle, San Antonio, TX 78249-0670, USA

ARTICLE INFO

Article history:
Received 16 May 2008
Received in revised form 28 November 2008
Accepted 2 December 2008
Available online 30 December 2008

Keywords:
Binary gas mixtures
In-tube turbulent convection
Artificial Neural Networks

ABSTRACT

Turbulent forced convection correlations are documented in the literature for air, gases and vapors ($Pr \sim 0.7$), for common liquids ($Pr > 1$) and for liquid metals ($Pr < 0.03$). In spite of this, there is a small gap in the Pr sub-interval between 0.1 and 1.0, which is occupied by binary gas mixtures. In this paper, data for turbulent forced convection for the in-tube flow have been gathered and a fully connected back-propagation Artificial Neural Network (ANN) is used to learn the pattern of Nu as a double-valued function of Re and Pr. The available data are separated in two subsets to train and test the neural network. A set with 80% of the data is used to train the ANN and the remaining 20% are used for testing. After the neural network is trained, we make use of the excellent nonlinear interpolation capabilities of ANNs to predict Nu for the sought range $0.1 < Pr < 0.7$ for Re between 10^4 and 10^6. These predictions are later extended to generate a comprehensive correlation for Re between 10^4 and 10^6 that aptly covers the complete spectrum of Prandtl numbers.

1. Introduction

The analysis of thermal systems using binary gas mixtures has been attracting more attention lately because of the improvement in performance due to the favorable thermodynamic and transport properties inherent to the binary gas mixtures compared to pure gases. For instance, binary gas mixtures are chemically inert and many noble gases have higher specific heat ratios and molecular weights compared to air. This characteristic has a definitive bearing on the improved heat transfer under similar operating conditions. It has been speculated that propulsion systems for space exploration as well as terrestrial power plants applications show performance improvements utilizing binary gas mixtures [1,2].

As indicated by Poling et al. [3], the prediction of the thermodynamic and transport properties of binary gas mixtures is a difficult subject because the nonlinear behavior of the thermophysical properties with respect to the mixture composition complicates the analysis. These authors mixed helium (He) as the primary light gas with seven secondary heavier gases that included carbon dioxide (CO_2), methane (CH_4), nitrogen (N_2), oxygen (O_2), sulfur hexafluoride (SF_6), tetrafluorumethane or carbon tetrafluoride (CF_4) and xenon (Xe) and obtained the respective properties of the mixtures. Shown in Fig. 1 is the family of the seven Prandtl number curves Pr_{mix} varying with the molar gas composition w inside the w-domain $[0, 1]$. The Pr_{mix} curves show that the left extreme of the abscissa $w = 0$ for the light He is associated with $Pr = 0.665$, whereas the right extreme $w = 1$ corresponds to multiple $Pr \sim 1$ representative of each of the heavier secondary gases. The Pr_{mix} are in ascending order: 0.669 for Xe, 0.715 for CH_4, 0.716 for O_2, 0.721 for N_2, 0.762 for CO_2, 0.8 for CF_4 and 1.511 for SF_6. As the molar mass difference between He (the light primary gas) and CO_2, CH_4, CF_4, SF_6, N_2, O_2 and Xe (the heavy secondary gases) increased, the magnitude of $Pr_{mix}(w)$ consistently diminished.

It is common to consider that three main sub-groups exist inside the Pr spectrum of viscous fluids: metallic liquids with $Pr \ll 1$; air, pure gases and vapors with $Pr \sim 1$; water and light liquids with $Pr \sim 10$; and oils and heavy liquids with $Pr \gg 1$. However, despite that the majority of practical applications in heat transfer engineering utilize air, water and oils having $Pr \geqslant 0.7$ collectively, certain binary gas mixtures with $0.1 < Pr < 0.7$ have attracted increasing attention. For instance, Campo et al. [4] studied five binary gas mixtures with the purpose of intensifying turbulent free convection from heated vertical plates to cold gases. Also, in recent years a variety of sophisticated industrial applications have been proposed and analyzed.

Turbulent heat transfer with fully developed gas flow inside tubes has been well documented in the literature [5–7]. Available correlations normally cover most of the Prandtl number spectrum. However, there is currently no correlation that covers the complete range of Prandtl numbers that embodies liquid metals, binary gas mixtures, pure gases, and common liquids including thick oils. In this paper we intend to generate such a correlation by first utiliz-

* Corresponding author. Tel.: +1 209 228 7858; fax: +1 209 228 4047.
E-mail address: gdiaz@ucmerced.edu (G. Diaz).

1290-0729/$ – see front matter
doi:10.1016/j.ijthermalsci.2008.12.001

Nomenclature

c_P	specific heat capacity
D	diameter
h	mean convective coefficient
k	thermal conductivity
L	length
Nu	mean Nusselt number, $\frac{hD}{k}$
Pr	Prandtl number, $\frac{\mu c_P}{k}$
Pr_{mix}	Prandtl number of binary gas mixture, $(\frac{\mu c_P}{k})_{\text{mix}}$
Re	Reynolds number, $\frac{\rho u D}{\mu}$
T	temperature
u	mean axial velocity
w	molar gas composition of binary gas mixture
w_{opt}	optimal molar gas composition of binary gas mixture
x_{hd}	hydrodynamic entrance length

Greek symbols

μ	dynamic viscosity
ρ	density

Subscripts

f	film
m	mean bulk
w	wall

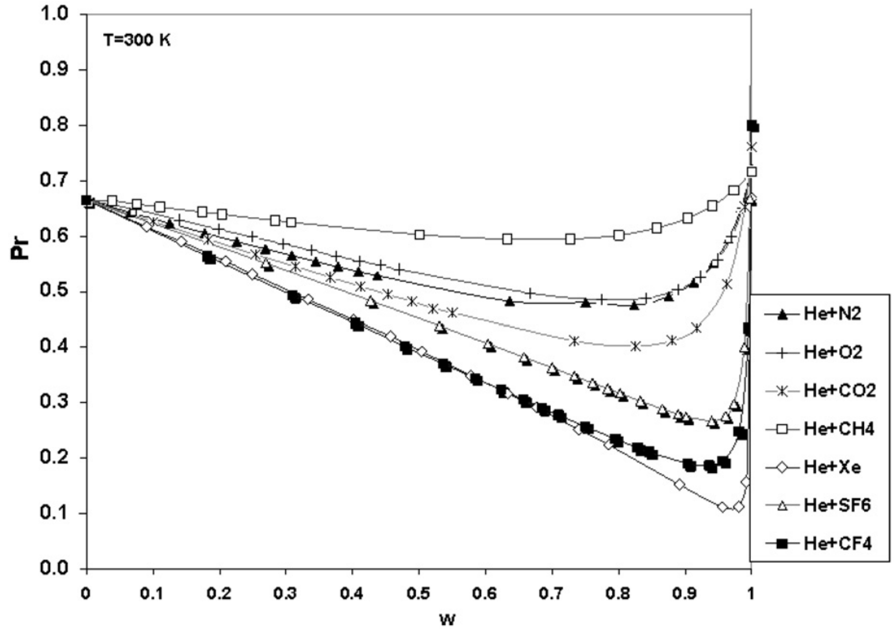

Fig. 1. Variation of the Prandtl number with the molar gas composition w for selected Helium-based binary gas mixtures at $T = 300$ K and $p = 1$ atm.

ing artificial neural networks to obtain a prediction for the range of Prandtl number between 0.001 and 1000 united with Reynolds number between 10^4 and 10^6.

From a historical perspective, the phasing out of halogenated halocarbons became effective at the end of 1995 by international agreement. The companion fluids HCFCs are suffering a similar fate, as they are considered controlled substances with a virtual phase-out by 2020. Thermoacoustic refrigerators are devices that convert sound energy into heat energy. As discussed by Herman and Travnicek [8], these devices pose some advantages over conventional refrigerators because they are environmentally friendly and simple in operation. Because they use gases such as, helium, xenon, and air, they do not affect the environment like hydrochlorofluorocarbons (HCFCs) and hydrofluorocarbons (HFCs) in conventional refrigerators. It has been demonstrated by Garrett et al. [9] and Tijani et al. [10] that a decrease in the Prandtl number of the gas flowing through the device improves the efficiency of thermoacoustic refrigerators. Essentially, these authors were referring to a specific type of gases that possess $Pr < 0.7$.

The Closed-Brayton-Cycle (CBC) is being considered by NASA as a candidate thermodynamic cycle for applications related to space power conversion for lunar and Mars surface missions [1]. The CBC can be integrated with various heat sources including solar heat receivers, radioisotope fuel sources, or fission reactors. The working fluids under consideration are binary gas mixtures. Because light Helium has the best thermal conductivity but a small molecular weight, mixing Helium (He) with heavier gases like Krypton (Kr) or Xenon (Xe) is twice beneficial. First, it increases slightly the heat transfer coefficient beyond that of He and second it decreases significantly the turbomachinery loading.

It is logical to think that aside from the potential application to thermoacoustic refrigerators and Combined Brayton Cycles (CBC) for space missions, binary gas mixtures may soon become candidate gases to remove moderate-to-large amounts of heat in applications of heat transfer engineering.

Artificial neural networks (ANNs) have been used in recent years to predict the behavior of steady state and dynamical systems in engineering. Thibault and Grandjean [11] provided an introduction to the use of ANNs in connection to heat transfer. Jambunathan et al. [12] employed ANNs to model one-dimensional transient heat conduction from measurements using liquid crystal thermography. Bittanti and Piroddi [13] utilized neural networks together with a generalized minimum variance control methodology for heat exchanger applications. Diaz et al. [14] applied ANNs to a series of problems of increasing complexity which included conduction, convection, and the prediction of experimental data of a cross-flow heat exchanger. The transient analysis of a single-tube heat exchanger involving a large number of local identical neural

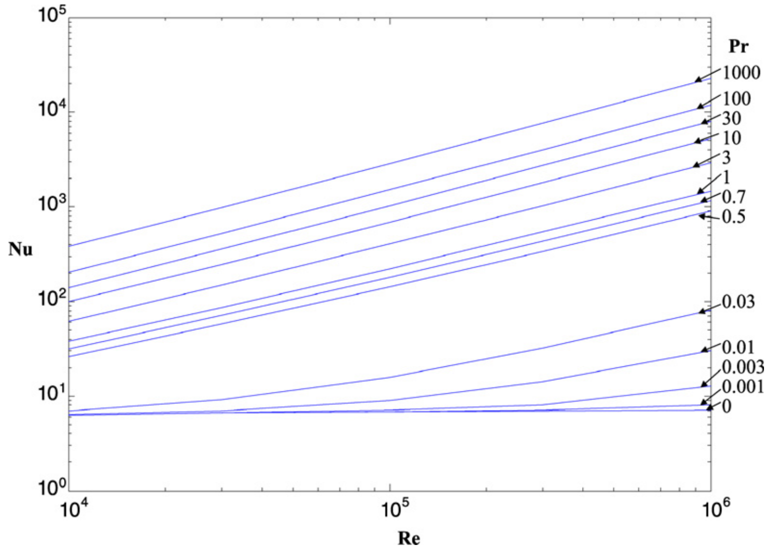

Fig. 2. Mean Nusselt number varying with the Reynolds and Prandtl numbers for fully developed turbulent flow in smooth tubes.

networks was performed by Lecoeuche et al. [15]. Su et al. [16] applied ANNs for the estimation of critical heat flux (CHF) in reference to nuclear fuel rods. They obtained an accuracy of $\pm 10\%$ in their predictions by training the neural network with local or CHF point conditions. CHFs were also analyzed by Zhang et al. [17] for flow boiling of water in mini channels with diameters ranging between 0.33 and 6.22 mm. Chen et al. [18] calculated heat transfer coefficients of supercritical carbon dioxide in a heat exchanger implementing modified radial basis function networks. Complex heat transfer predictions in humid air-water heat exchangers were performed by Pacheco-Vega et al. [19] via ANNs and suitable correlations.

In this paper we utilized artificial neural networks to compile values of the mean Nusselt number particularized to binary gas mixtures in the Prandtl number sub-region $(0.1, 1)$. Thereafter, these values are used to generate a heat transfer correlation that is obtained from using a combination of available data and predicted values.

2. Turbulent forced convection

Although there is no satisfactory general expression for the entry length in turbulent pipe flow x_{hd}, as a first approximation, the inequality described by Eq. (1)

$$10 \leqslant \frac{x_{\mathrm{hd}}}{D} \leqslant 60 \tag{1}$$

serves as a guidance [5].

In the past, several authors have developed theoretical and experimental studies to describe the variation of the mean Nusselt number with respect to Reynolds and Prandtl numbers in fully developed turbulent flow inside circular tubes. The most representative work was carried out by Kays and Leung [20] and Leung et al. [21] and the results are summarized in Fig. 2.

Different correlations that cover specific ranges of Reynolds and Prandtl numbers have been reported in the literature [5–7]. For liquid metals with $Pr < 0.1$ the following correlation has been recommended for constant heat flux on the wall [7]:

$$Nu_{D,m} = 6.3 + 0.0167\, Re_{D,f}^{0.85}\, Pr_w^{0.93} \tag{2}$$

where m, f, and w denote the mixing-cup, film, and wall temperatures, respectively. This correlation gives results within 10% of measurements. For the range of Prandtl number between 0.5 and 1.0

$$Nu = 0.022\, Re^{0.8}\, Pr^{0.6} \tag{3}$$

has been suggested in [5]. For Reynolds number in the range between 10^4 and 1.2×10^5 and Prandtl between 0.6 and 120, the well-known correlation by Dittus–Boelter [22] is commonly used for liquids and gases:

$$Nu = 0.023\, Re_D^{0.8}\, Pr^n \tag{4}$$

where $n = 0.4$ for heating and $n = 0.3$ for cooling. Eq. (4) gives results that can be 20% high for gases and 40% low for water at high Reynolds numbers [7]. The more recent Gnielinski [23] equation

$$Nu = 0.0214(Re^{0.8} - 100)\, Pr^{0.4} \tag{5}$$

for $0.5 < Pr < 1.5$ and $10^4 < Re < 10^6$, is being used extensively for minichannels and has uncertainties of 6%. This equation is applicable for binary gas mixtures with $Pr > 0.5$ only.

3. Binary gas mixtures

Existing theoretical and experimental data from [5,24] were used by Kirov and Kozhelupenko [25] to obtain a correlation that approximates the mean Nusselt number in the range of Prandtl between 0.3 and 1.0 with the Reynolds number varying from 10^5 to 10^7. They proposed a correlation with the exponent of the Pr number being a function of the Prandtl number as shown by Eq. (6).

$$Nu = 0.022\, Re^{0.8}\, Pr^k \tag{6}$$

where $k = 0.595\, Pr^{-0.126}$. This expression agrees within 1% with the solution obtained by using Lyon's integral [24,26]. The same authors proposed a simplified expression that embodies a 5% of error with a constant exponent for the Prandtl number, as described by Eq. (7) [25].

$$Nu = 0.022\, Re^{0.8}\, Pr^{0.68} \tag{7}$$

This is very similar to the correlation recommended in [5]

$$Nu = 0.022\, Re^{0.8}\, Pr^{0.6} \tag{8}$$

The correlation by Sleicher and Rouse [27] given by Eq. (9) is also recommended for a range of Prandtl number between 0.1 and 10^5 together with Reynolds numbers in the range $10^4 < Re < 10^6$.

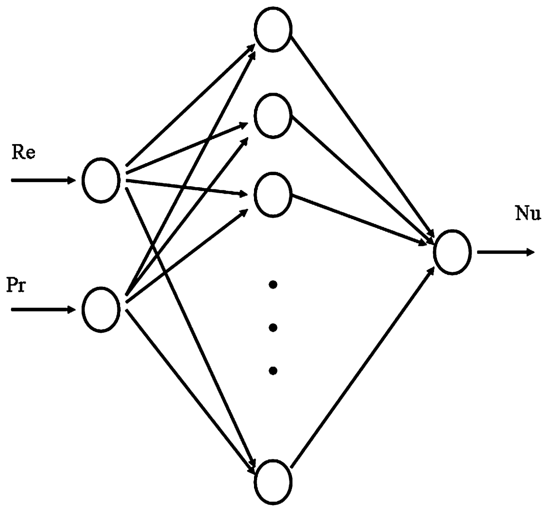

Fig. 3. Schematic representation of an artificial neural network involving *Nu*, *Re* and *Pr*.

$$Nu = 5 + 0.015\, Re^a\, Pr^b \tag{9}$$

where $a = 0.88 - \frac{0.24}{4+Pr}$ and $b = \frac{1}{3} + 0.5\exp(-0.6\,Pr)$. This correlation provides a level of accuracy within 10% [7].

Currently there is no comprehensive correlation for the mean Nusselt number that covers the entire range of Reynolds and Prandtl numbers shown in Fig. 2. The central objective of this paper is to develop such a correlation by means of using artificial neural networks.

4. Artificial neural network model

A fully-connected sigmoid-activation-function artificial neural network is sketched in Fig. 3 having an input layer with two nodes, a hidden layer of nodes, and an output layer with one node. The neural network was implemented to perform a nonlinear interpolation of available data representative of the mean Nusselt number, *Nu*, as a double-valued function of the Reynolds number, *Re*, and Prandtl number, *Pr*. Data were obtained from [5,20,25] and from more recent results by Heng et al. [28] and Yu et al. [29]. The heat transfer data obtained from these references came from various sources: (1) asymptotic solutions based on empirical values of velocity and eddy diffusivity [5,20], (2) the exact solution using Lyon's integral [25,26], (3) numerical solutions that utilize a theoretically based algebraic correlation for the time-averaged turbulent shear stress and a purely empirical correlation for the heat flux density [28,29]. The Reynolds number for fully turbulent flow varied between 10^4 and 10^6. The data provided to the ANN covered *Nu*–*Re* pairs of discontinuous values of Prandtl number that extend from 0.001 to 1000. Thereafter, the data collection was divided into two subsets; one that contains 80% of the original data that was used for training the ANN. The other subset with the remaining 20% of the data was employed for testing and validation of the predicted values of *Nu*. A backpropagation training algorithm served as the vehicle in the analysis due primarily to its excellent generalization properties [30].

As noted by Lee and Lam [31], the structure of the neural network is obtained by using an algorithm that minimizes the maximum error in the prediction of the test data by changing the number of nodes in the single hidden layer. Plotted in Fig. 4 is the normalized error of the test data varying with respect to the number of nodes in the hidden layer. It is clearly observed that no improvement is manifested in the prediction by having more than seven nodes in the hidden layer.

After the training process was completed the ANN was used to predict the values of *Nu* for the entire region of Reynolds and Prandtl numbers, i.e. $10^4 \leqslant Re \leqslant 10^6$ and $10^{-3} \leqslant Pr \leqslant 10^3$. Fig. 5 shows the results of the prediction, Nu_{ANN}, plotted with respect to the available data, Nu_{data}. The complete set of predicted values remained within ±15% of the available data.

It can be observed that the ANN captures the trend of the data satisfactorily. In addition, it is seen that the ANN is capable of predicting the mean Nusselt number of turbulent flow in a smooth pipe for the complete range of Reynolds and Prandtl numbers shown in Fig. 2. The ANN was then used to predict values of the mean Nusselt number at a number of points inside the range $0.1 \leqslant Pr \leqslant 0.7$ for turbulent Reynolds numbers between 10^4 and 10^6. Fig. 6 is presented as a supplementary summary of the combined data taken from Fig. 2 (solid lines) and the new predicted *Nu* values furnished by ANN for $0.1 < Pr < 0.7$ (dashed lines).

5. Development of a correlation

Although computer simulations of thermal systems are quite common nowadays, the utilization of artificial neural networks for

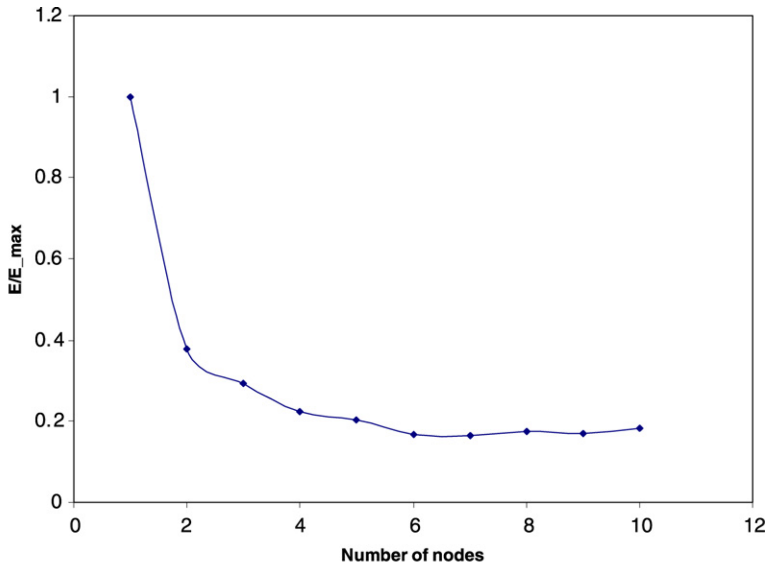

Fig. 4. Decay of the normalized error with the number of nodes.

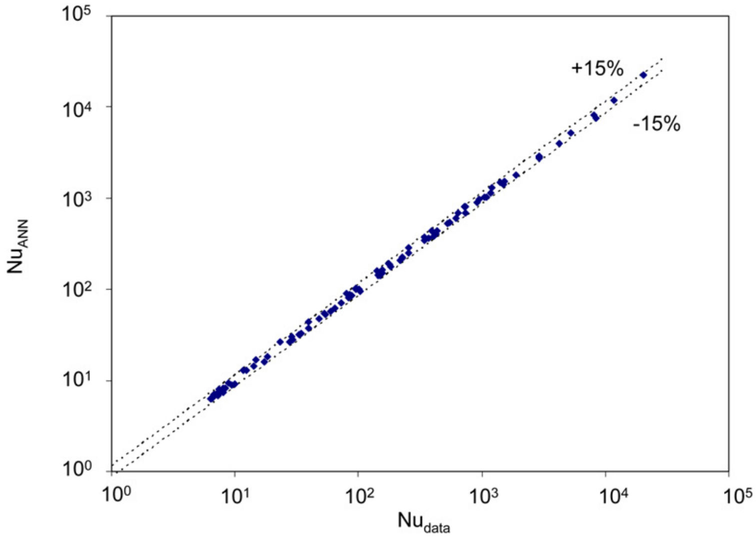

Fig. 5. Nusselt number predicted by ANN versus *Nu* from the available data for *Pr* between 10^{-3} and 10^{3} and *Re* between 10^{4} and 10^{6}.

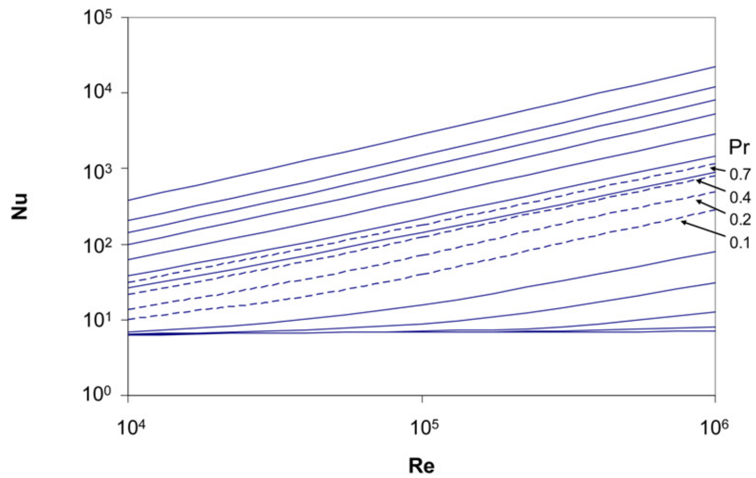

Fig. 6. Mean Nusselt number as a function of Reynolds and Prandtl numbers including the prediction with ANN for $0.1 < Pr < 0.7$.

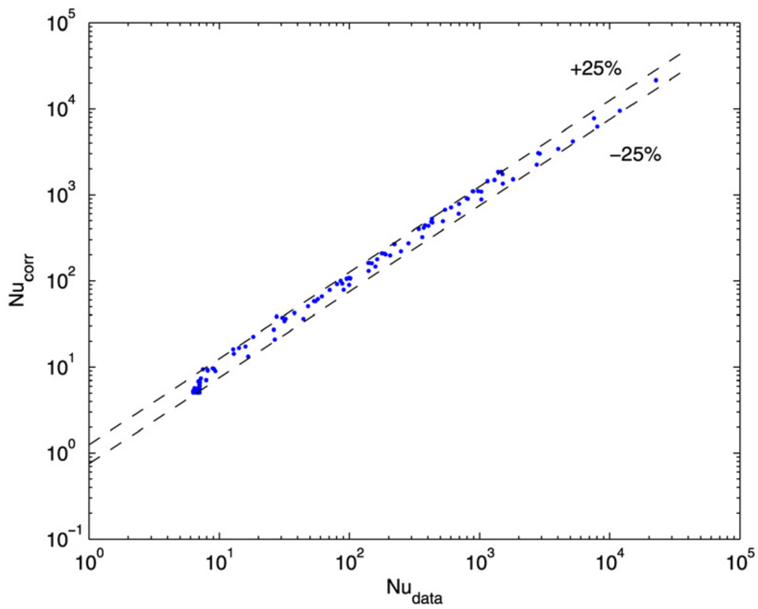

Fig. 7. Nusselt predicted by correlation versus *Nu* from the available data for *Pr* between 10^{-3} and 10^{3} and *Re* between 10^{4} and 10^{6}.

the prediction of Nusselt numbers or heat transfer rates continues to be less widespread than the use of analytical expressions in the form of correlations that predict the behavior of Nu as a function of the Reynolds and Prandtl numbers. For this purpose, the predicted values obtained with the ANN for the range of Prandtl number between 0.1 and 0.7 were merged with the rest of the available data used for training and testing the ANN with the intention of obtaining an expression that will predict Nu covering the complete range of Re and Pr analyzed in this study.

The collection of results, shown in Fig. 2, shows that the slopes of the upper sub-family of curves for $Pr \geqslant 1$ are nearly equal regardless the value of Re. This behavior justifies the functional relation $Nu = F(Re, Pr) = F_1(Re) \times F_2(Pr)$ that leads to the conventional power-law correlation of the form $C\,Re^n\,Pr^m$. Conversely, for the lower sub-family of curves with $Pr \ll 1$, the slopes change significantly with increments in Re and Pr, strongly suggesting a more involved correlation of the form $C_1 + C_2\,Re^n\,Pr^m$. Also, for the range of Prandtl numbers between 0.1 and 0.7, it has been suggested that the exponent of Pr should be a function of the Prandlt number [25]. Following the structure of the correlation proposed in [27] we utilize an unconstrained nonlinear optimization algorithm to obtain the coefficients of the new correlation. The resulting expression is given by Eq. (10):

$$Nu = 5.0742 + 0.0153\,Re^{0.8470}\,Pr^{a} \tag{10}$$

where the exponent $a = 0.3556 + 0.5257\exp(-0.5868\,Pr)$.

Fig. 7 shows the prediction of Nu based on the new correlation with respect to the original Nu data. It is verified that the correlation predicted 92% of the data within $a \pm 25\%$ margin. Although the correlation shows a larger uncertainty with respect to the prediction obtained with the ANN, the simplicity of the expression and its easy implementation favors the correlation.

6. Conclusions

Data for turbulent forced convection for the in-tube flow have been gathered, analyzed and modeled by means of powerful artificial neural networks. The ANN is used to predict the in-tube turbulent forced convection in the specific range of Prandtl number corresponding to binary gas mixtures ($0.1 < Pr < 0.7$). The complete set of data is utilized afterwards to generate a comprehensive correlation that covers the vast range of Reynolds number between 10^4 and 10^6 in conjunction with a large Pr number spectrum contained in $0.001 < Pr < 1000$. The correlation predicts the entire set of data with an accuracy of $\pm 25\%$.

References

[1] M.S. El-Genk, J.-M. Turnier, Noble-gas binary mixtures for closed-Brayton-cycle space reactor power systems, J. Propulsion and Power 23 (4) (2007) 863–873.

[2] M.S. El-Genk, J.-M. Tournier, Noble gas binary mixtures for gas-cooled reactor power plants, Nuclear Engineering and Design 238 (2008) 1353–1372.

[3] B.E. Poling, J.M. Prausnitz, J.P. O'Connell, The Properties of Gases and Liquids, McGraw-Hill, New York, 2001.

[4] A. Campo, S. Chikh, S.S. Sablani, Optimal molar gas composition of selected gas mixtures with helium that maximize turbulent free convection along vertical plates, J. Fluids Eng. 128 (1) (2006) 199–201.

[5] W.M. Kays, Convective Heat and Mass Transfer, McGraw-Hill, New York, 1966.

[6] A. Bejan, Convection Heat Transfer, 3rd ed., John Wiley & Sons, New York, 2004.

[7] L.C. Burmeister, Convective Heat Transfer, John Wiley & Sons, New York, 1983.

[8] C. Herman, Z. Travnicek, Cool sound: the future of refrigeration? Thermodynamic and heat transfer issues in thermoacoustic refrigeration, Heat Mass Transfer 42 (2006) 492–500.

[9] S.L. Garrett, J.A. Adeff, T.J. Hofler, Thermoacoustic refrigerator for space applications, J. Thermophys. Heat Transfer 7 (1993) 595–599.

[10] M.E.H. Tijani, C.H. Zeegers, A.T.A.M. de Waele, Prandtl number and thermoacoustic refrigerators, J. Acoust. Soc. Am. 112 (1) (2002) 134–143.

[11] J. Thibault, B. Grandjean, A neural network methodology for heat transfer data analysis, Int. J. Heat Mass Transfer 34 (1991) 2063–2070.

[12] K. Jambunathan, S.L. Hartle, S. Ashforth-Frost, V.N. Fontama, Evaluating convective heat transfer coefficient using neural networks, Int. J. Heat Mass Transfer 39 (11) (1996) 2329–2332.

[13] S. Bittanti, L. Piroddi, Nonlinear identification and control of a heat exchanger: a neural network approach, J. Franklin Inst. 334 (1) (1997) 135–153.

[14] G. Diaz, M. Sen, K.T. Yang, R.L. McClain, Simulation of heat exchanger performance by artificial neural networks, Int. J. HVAC&R Research 5 (1999) 195–208.

[15] S. Lecoeuche, S. Lalot, B. Desmet, Modelling a non-stationary single-tube heat exchanger using multiple coupled local neural networks, Int. Commun. Heat Mass Transfer 32 (7) (2005) 913–922.

[16] G.H. Su, K. Fukuda, D. Jia, K. Morita, Application of an artificial neural network in reactor thermo-hydraulic problem: prediction of critical heat flux, J. Nucl. Sci. Tech. 39 (5) (2002) 564–571.

[17] W. Zhang, T. Hibiki, K. Mishima, Y. Mi, Correlation of critical heat flux for boiling of water in mini-channels, Int. J. Heat Mass Transfer 49 (5–6) (2006) 1058–1072.

[18] J. Chen, K.-P. Wang, M.-T. Liang, Predictions of heat transfer coefficients of supercritical carbon dioxide using the overlapped type of local neural network, Int. J. Heat Mass Transfer 48 (12) (2005) 2483–2492.

[19] A. Pacheco-Vega, G. Diaz, M. Sen, K.T. Yang, R.L. McClain, Heat rate predictions in humid air-water heat exchangers using correlations and neural networks, J. Heat Transfer 123 (2) (2001) 348–354.

[20] W.M. Kays, Y. Leung, Heat transfer in annular passages- hydrodynamically developed turbulent flow with arbitrarily prescribed heat flux, Int. J. Heat Mass Transfer 6 (1963) 537–557.

[21] E.Y. Leung, W.M. Kays, W.C. Reynolds, Heat transfer in annular passages with hydrodynamically developed turbulent flow, Report AHT-4, Dept. of Mechanical Engineering, Stanford University, 1962.

[22] R.H.S. Winterton, Where did the Dittus and Boelter equation come from? Int. J. Heat Mass Transfer 41 (4–5) (1998) 809–810.

[23] V. Gnielinski, New equations for heat and mass transfer in turbulent pipe and channel flow, Int. Chem. Eng. 16 (1976) 359–368.

[24] S.S. Kutateladze, in: R.D. Cess (Ed.), Fundamentals of Heat-Transfer, Edward Arnold (Publishers) Ltd., London, 1963.

[25] V.S. Kirov, Y.D. Kozhelupenko, S.D. Tetel'baum, Determination of heat-transfer coefficient for gas mixtures containing helium and hydrogen, J. Eng. Physics and Thermophysics 26 (2) (1974) 152–154.

[26] R.N. Lyon, Liquid metal heat-transfer coefficients, Chem. Eng. Prog. 47 (2) (1951) 75–79.

[27] C.A. Sleicher, M.W. Rouse, A convenient correlation for heat transfer to constant and variable property fluids in turbulent pipe flow, Int. J. Heat Mass Transfer 18 (5) (1975) 667–683.

[28] L. Heng, C. Chan, S.W. Churchill, Essentially exact characteristics of turbulent convection in a round tube, Chem. Eng. J. 71 (1998) 163–173.

[29] B. Yu, H. Ozoe, S.W. Churchill, The characteristics of fully developed turbulent convection in a round tube, Chem. Eng. Sci. 56 (2001) 1781–1800.

[30] D.E. Rumelhart, G.E. Hinton, R.J. Williams, Learning Internal Representations by Error Propagation. Parallel Distributed Processing. Exploration in the Microstructure of Cognition, MIT Press, Cambridge, MA, 1986.

[31] K.W. Lee, H.N. Lam, Optimal sizing of feed-forward neural networks: Case studies, in: Proc. 2nd New Zealand Two-Stream International Conference on Artificial Neural Networks and Expert Systems, 1995, pp. 79–82.